Severe Plastic Deformation by Machining Characterized by Finite Element Simulation

M. SEVIER, H.T.Y. YANG, S. LEE, and S. CHANDRASEKAR

A finite element model of large strain deformation in machining is presented in the context of using machining as a controlled method for severe plastic deformation (SPD). Various characteristics of the large strain deformation field associated with chip formation, including strain, strain distribution, strain rate, and velocity field, are calculated using the model and compared with direct measurements in plane strain machining. Reasonable agreement is found for all cases considered. The versatility and accuracy of the finite element model are demonstrated, especially in the range of highly negative rake angles, wherein the shear plane model of machining is less applicable due to the nature of material flow around the tool cutting edge. The influence of the tool rake angle and friction at the tool-chip interface on the deformation is explored and used to establish correspondences between controllable machining input parameters and deformation parameters. These correspondences indicate that machining is a viable, controlled method of severe plastic deformation. Implications of the results for creation of nanostructured and ultra-fine-grained alloys by machining are briefly highlighted.

DOI: 10.1007/s11663-007-9103-9

I. INTRODUCTION

A commonly used approach for refinement of microstructure in metals and alloys is severe plastic deformation (SPD).[1–3] Severe plastic deformation generally refers to a class of processes wherein a material is deformed to large plastic strains (> 3) through the use of multiple passes of deformation. The role of severe plastic deformation in microstructure refinement is best highlighted in the pioneering studies of Embury and Fisher[4] on deformation of pearlite, and Langford and Cohen[5] on iron. Langford and Cohen,[5] for example, imposed large plastic strains in iron by repeated passes of wire drawing and found the microstructure of the deformed iron wire to be composed of grains and dislocation substructures with sizes in the sub-micrometer range. Furthermore, there was a significant increase in the flow stress of the wire. More recently severe plastic deformation has become the preferred route for producing bulk nanostructured materials.[1,3,6]

Two conventional severe plastic deformation procedures are equal channel angular pressing (ECAP)[1,3,6] and high pressure torsion (HPT).[1] In equal channel angular, a pressing sample is extruded repeatedly through a rigid die with a bend that imposes shear on the material. The cross sections of the die at the inlet and exit are kept the same so that the sample does not undergo any shape change. The sample material typically experiences a shear strain of 1 to 2 per pass and multiple passes of deformation are used to impose large strains and achieve refinement of the microstructure. In high pressure torsional straining, a thin circular disk is subjected to shear under superimposed normal pressure applied between a die and a rotating shaft. The shear is transmitted to the disk sample by friction as the shaft is rotated with respect to the die, thereby imposing large strains in the material. The resulting strain distribution is quite inhomogeneous through the thickness and along the radius of the sample.

While conventional severe plastic deformation studies have provided insights into mechanisms of microstructure refinement in metals and alloys of low initial strength, they do possess some limitations. First, multiple stages of deformation are needed to create the large plastic strains. Second, moderate and high-strength metals and alloys are difficult to deform at near-ambient temperatures in this manner due to constraints imposed by the forming equipment, including durability of tools and dies. Last, there are uncertainties pertaining to knowledge and control of deformation field parameters.

A potentially attractive route for imposing large plastic strains and strain rates in a single pass of deformation, while overcoming the aforementioned limitations, is the process of chip formation by machining. In contrast to rolling, extrusion, equal channel angular pressing and high pressure torsional straining, machining can impose uniform strains that are sufficiently large to realize ultra-fine-grained microstructures in the chip in only one pass.[7–9] Furthermore, machining can be used for severe plastic deformation of metals and alloys of high initial strength at various strain rates ranging from low to high.[8,10] The development of machining as a controlled method of severe plastic

M. SEVIER, Graduate Student, and H.T.Y. YANG, Professor, are with the Department of Mechanical Engineering, University of California, Santa Barbara, CA 93106, USA. Contact e-mail: henry.yang@chancellor.ucsb.edu S. LEE, Graduate Student, and S. CHANDRASEKAR, Professor, are with the Center for Materials Processing and Tribology, School of Industrial Engineering, Purdue University, West Lafayette, IN 47907-2023, USA.

Manuscript submitted March 8, 2007.
Article published online November 29, 2007.

deformation will be greatly facilitated if a correspondence can be established between deformation parameters and input machining parameters (Figure 1). Such a correspondence, in conjunction with experimental data, will build a relationship between input parameters, such as cutting speed, friction, rake angle, material properties, and the resulting microstructure and properties of metallic materials. The present study describes an initial attempt to establish this correspondence for plane strain machining using finite element simulation.

A. *Plane Strain Machining*

Plane strain (two-dimensional) machining offers attractive advantages as a method of severe plastic deformation because a single pass of deformation is sufficient to impose uniform effective strains of 1 to 10 in the chip. Furthermore, the strain rate can be varied over a wide range from 1 to 10^5/s. The geometry of machining in this simple manifestation (*i.e.*, plane strain machining (Figure 2)) is characterized by a sharp, wedge-shaped tool that removes a preset depth of material (a_o) as it translates parallel to the surface of the workpiece.[10,11] Chip formation occurs by concentrated shear within a narrow deformation zone often idealized as a "shear plane."[11–13] Grain refinement occurs as a direct consequence of the large shear strains imposed within this zone.[8,9]

In the shear plane model of machining, the resultant deformation is uniquely determined by the tool rake angle (α) and shear plane angle (ϕ); in fact, this model is an upper bound model for machining.[14] The shear strain (γ) can be obtained from measurements of a_o and a_c as follows:

$$\gamma = \frac{\cos\alpha}{\sin\phi\cos(\phi-\alpha)} \qquad [1]$$

$$\tan\phi = \frac{\frac{V_c}{V_o}\cos\alpha}{1-\frac{V_c}{V_o}\sin\alpha} = \frac{\frac{a_o}{a_c}\cos\alpha}{1-\frac{a_o}{a_c}\sin\alpha} \qquad [2]$$

where V_o and V_c are the workpiece and chip velocity, respectively (Figure 2(a)).

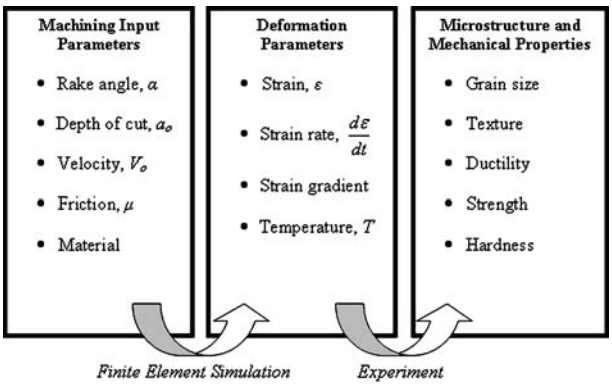

Fig. 1—Relationship between machining input parameters, deformation field parameters, and microstructure/mechanical properties.

It is apparent from Eqs. [1] and [2] that the strain can be readily varied by modifying the tool rake angle (α), an input machining parameter. Because the shear plane model assumes all of the strain imposed in the chip to arise from simple shear, the corresponding effective strain (ε_{eff}) is given by

$$\varepsilon_{eff} = \left(\frac{2}{3}\varepsilon_{ij}\varepsilon_{ij}\right)^{1/2} = \frac{\gamma}{3^{1/2}}, \qquad [3]$$

or

$$\varepsilon_{\text{eff}} = \frac{\cos\alpha}{3^{1/2}\cdot\sin\phi\cos(\phi-\alpha)}. \qquad [4]$$

In machining, unlike conventional severe plastic deformation methods, the thickness (and geometry) of deformed material (chip) at the exit of the deformation zone is not defined *a priori*. For example, the same rake angle (α) may produce different values of strain in different materials depending on the associated shear angle (ϕ); this shear angle is not a controllable input parameter. Additionally, the friction at the tool-chip interface influences the shear angle and the strain. This friction may be varied, for example, by use of tool coatings and modulation of the tool-chip contact. The temperature and strain rate in the deformation zone are dependent mainly upon the cutting speed. The relation between controllable machining input parameters such as α, a_o, and V_o, and deformation parameters (*e.g.*, strain and strain rate) (Figure 1) can be established by experiment.[10] Alternatively, this can be computed using the finite element method. If such a relation is firmly established, then it will be possible to impose any desired shear strain, within limits, in the chip by suitably adjusting the controllable machining parameters. It should be noted that because the shear plane model is essentially an upper bound analysis of the chip formation process,[14] details regarding the geometry of the deformation are not provided.

The present study describes a finite element simulation to characterize strain and strain rates within the deformation zone as a function of rake angle and friction in the low speed cutting of metals. Temperature is not an important parameter in the present study because heat generation is expected to be insignificant at the low cutting speeds.[11,12] The predicted deformation parameters are compared with measurements. The results are of direct relevance to development of machining as a method of severe plastic deformation and for understanding microstructure evolution during deformation (Figure 1).

B. *Experimental Results*

The deformation zone in plane strain machining of metals has recently been characterized using high-speed photography in conjunction with an image analysis technique, *viz*. particle image velocimetry (PIV).[10] This technique has been extensively used in fluid mechanics to map velocity fields in fluid flow by tracking the motion of tracer particles dispersed in the fluid. In plane

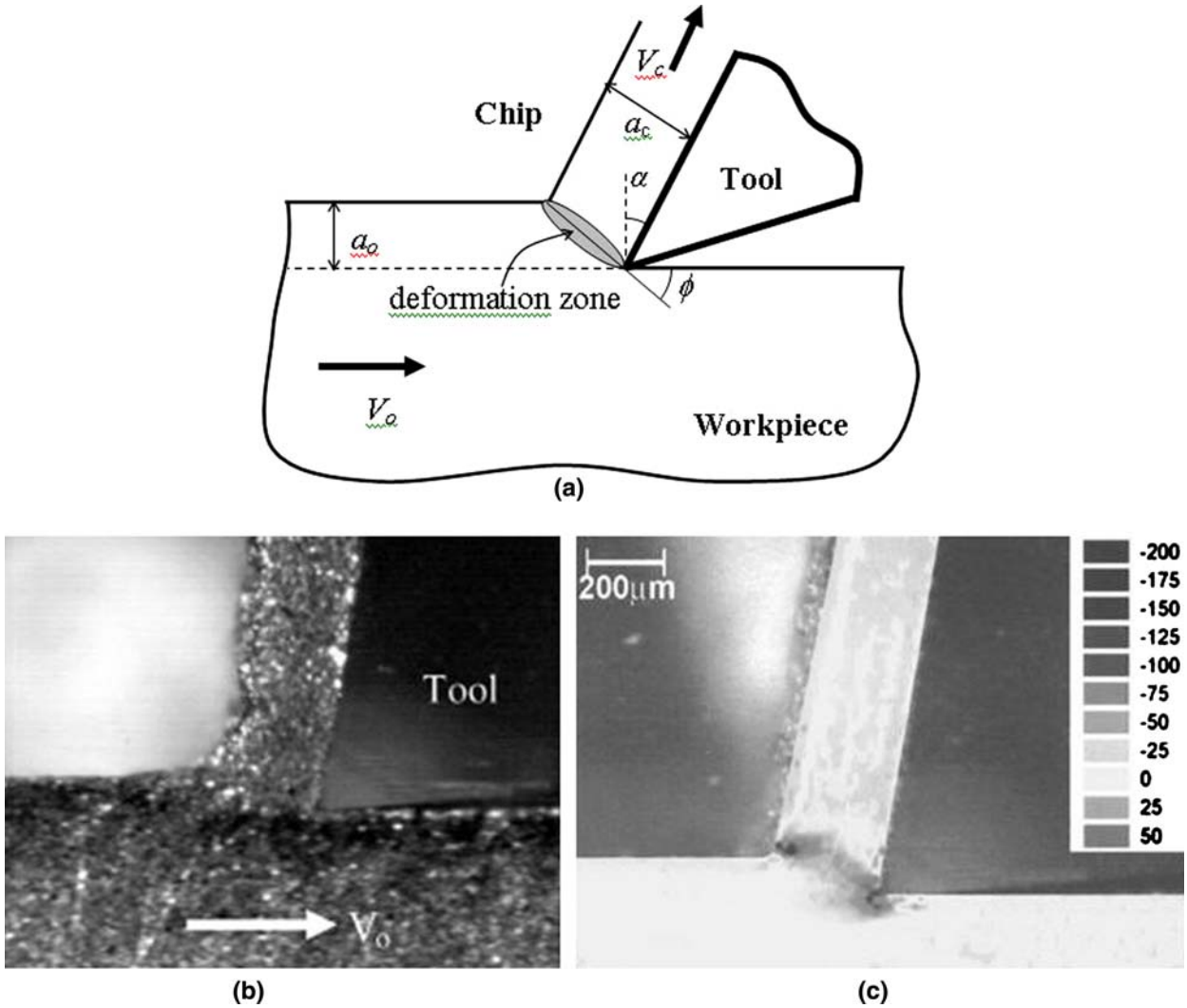

Fig. 2—(*a*) Schematic of plane strain machining, (*b*) asperities on workpiece surface used in PIV analysis, and (*c*) example of strain rate distribution in plane strain machining obtained by PIV.

strain machining, the function of tracer particles is served by asperity-like features created on a side of the workpiece by abrasion or sand blasting (Figure 2(b)), which scatter light significantly different than the surrounding regions in the metal. By measuring the displacement of these features over time using high-speed photography, velocity, strain rate, and strain data in the deformation zone, chip and workpiece subsurface can be obtained.[8,10] Experimental details pertaining to the application of PIV to machining can be found in References 8 and 10. Figure 2(c) is an example of strain rate distribution in the deformation zone obtained using the PIV analysis in low-speed machining of lead. Because strain rate is a measure of the incremental strain imposed over a finite time-step associated with incremental advancement of the tool, the distribution of strain rate in Figure 2(c) provides a direct characterization of the size and extent of the deformation zone. It is seen from this figure that the deformation zone is nonplanar and has finite width. Similar conclusions have been arrived at in prior studies using quick-stop and related observations.[12,13] Furthermore, the PIV analysis has shown that the cumulative strain imposed in the chip varies for different materials at the same tool rake angle. These observations highlight the need for modeling of the chip formation process to relate machining parameters (*e.g.*, rake angle, velocity, and friction) to deformation parameters (*e.g.*, strain, strain rate, and temperature) (Figure 1).

An important consequence of large strains imposed in the chip is formation of a range of ultra-fine-grain and nanoscale microstructures. This is seen in Figure 3 for pure oxygen free high conductivity (OFHC) copper subjected to different levels of plastic strain by varying the tool rake angle.[9] The nature of the microstructure is seen to be strongly dependent on the strain. In particular, a switchover from elongated subgrain to nanoscale equiaxed grain structures, with a significant fraction of high-angle grain boundaries, is observed at the higher levels of strain (Figure 3). This transition, which typically occurs at a critical value of strain, is controllable in various alloys by varying the deformation conditions.

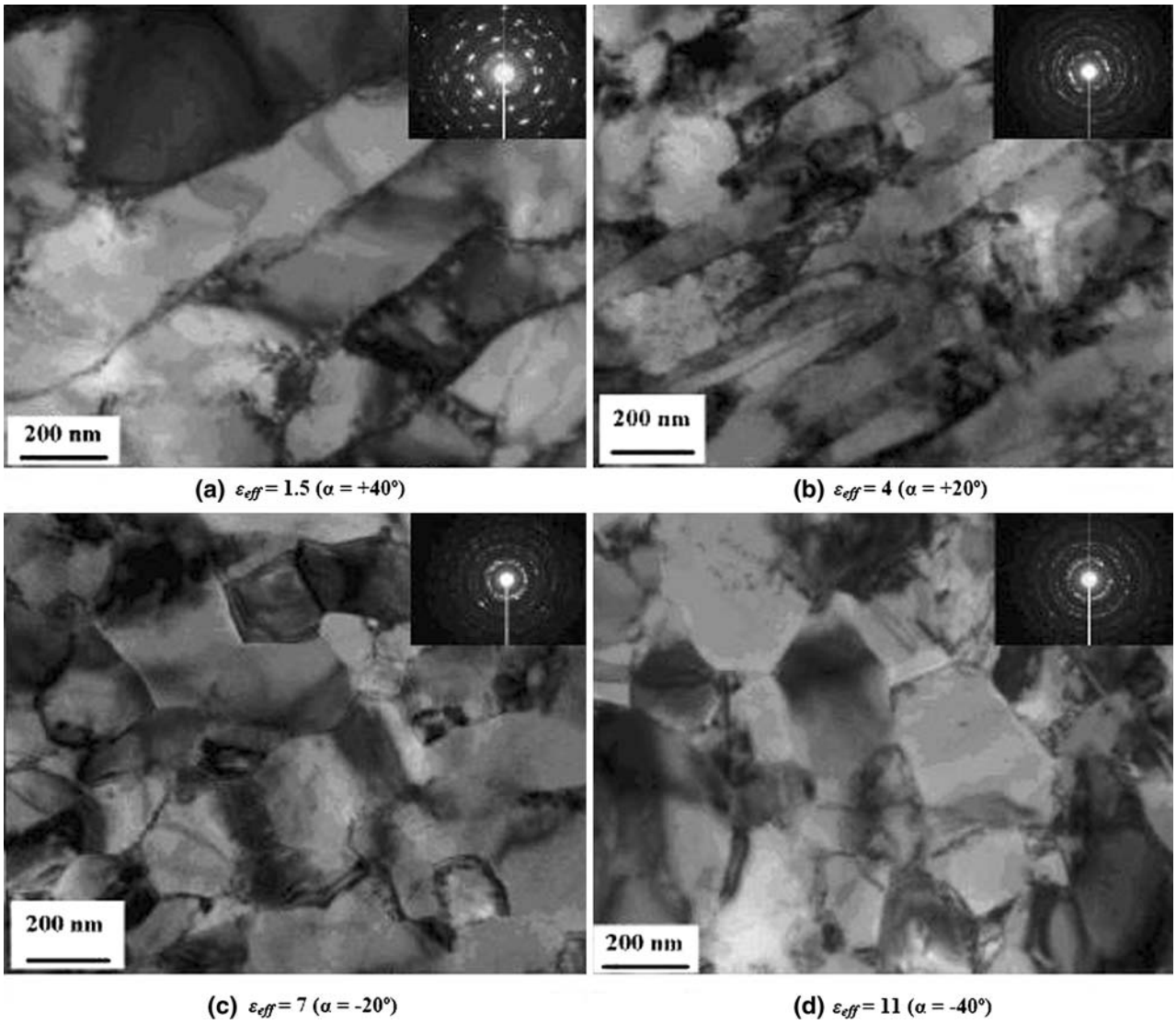

Fig. 3—Transmission electron micrographs of chips cut from pure (OFHC) copper with different values of effective strain (ε_{eff}).

Again, effective modeling would enable control of chip microstructures by predicting the machining parameters required to produce predetermined ultra-fine-grained morphologies. Such modeling is possible through the use of the finite element method.

II. FINITE ELEMENT MODELS FOR MACHINING

A. *Previous Models*

The finite element method has been widely used to study machining processes. Klamecki's model[15] was limited to the incipient cutting stage. Shirakashi and Usui[16] assumed a steady-state chip geometry and advanced the tool incrementally. Strenkowski and Carroll[17] were the first to model actual chip formation by having the nodes separate along a predefined "parting line." Other researchers have followed in their path with the nodes "unhooked" according to various limiting criteria imposed somewhat arbitrarily (strain, distance from the tool tip, *etc.*).[18–22] However, in simulating chip formation as tensile rupture rather than plastic flow as indicated by experiment,[23,24] these models may be somewhat inaccurate in their prediction of deformation parameters. Furthermore, these early studies encountered difficulty in simulating cutting with large negative rake angles.[25]

In order to effectively model extreme plastic deformation involved in chip formation while maintaining mesh continuity, subsequent studies have used adaptive meshing. Carroll and Strenkowski[26] adapted an Eulerian reference frame wherein the mesh is held constant while a viscoplastic material flows through the given control volume. Through iterative modification the eventual chip geometry could be determined as well as the forces. Sekhon and Chenot[27] used a similar flow formulation with the addition of automatic remeshing to reflect changes in chip geometry.

In 1995, the International Academy of Production Engineering (CIRP) established a working group ''Modelling of Machining Operations'' with the goal of advancing machining modeling techniques so that they would be capable for use in industry. Current state of the art of modeling in machining has been well-addressed in keynote publications by members of this group.[28,29] One such direction developed by Ceretti *et al.*[30] applies element deletion to the process of chip formation. In this type of simulation, elements having reached a critical value of accumulated damage are subsequently removed from the analysis. Recently, this technique has been successfully applied to simulate the formation of serrated or segmented chips, such as when machining a heterogeneous material[31] or when using a negative rake angle.[32]

Another direction for finite element development, more pertinent to the model presented in this study, involves Lagrangian mesh formulation with iterative remeshing.[33,34] To address computational time concerns due to the periodic remeshing, researchers have applied an arbitrary Lagrangian Eulerian (ALE) formulation to the machining process.[35–37] In this type of analysis, the nodal points of the finite element mesh may have degrees of freedom constrained by either material location (Lagrangian), spatial location (Eulerian), or an arbitrary motion defined by the analyst. This method allows for plastic flow to occur about the cutting tool tip while consistently maintaining a satisfactory aspect ratio for the elements, making this technique particularly convenient for simulating a wide range of tool rake angles.[38] Because machining has long been considered a process for making components, prior analyses have focused mainly on characterizing parameters of the workpiece surface and machining forces and paid much less attention to predicting deformation characteristics of the chip, the focus of this study.

B. *Current Finite Element Approach*

The present simulation is aimed at predicting deformation associated with chip formation and its dependence on the controllable machining parameters. For this purpose, a finite element model of plane strain machining has been constructed for the case of an elastic, perfectly-plastic material undergoing plane

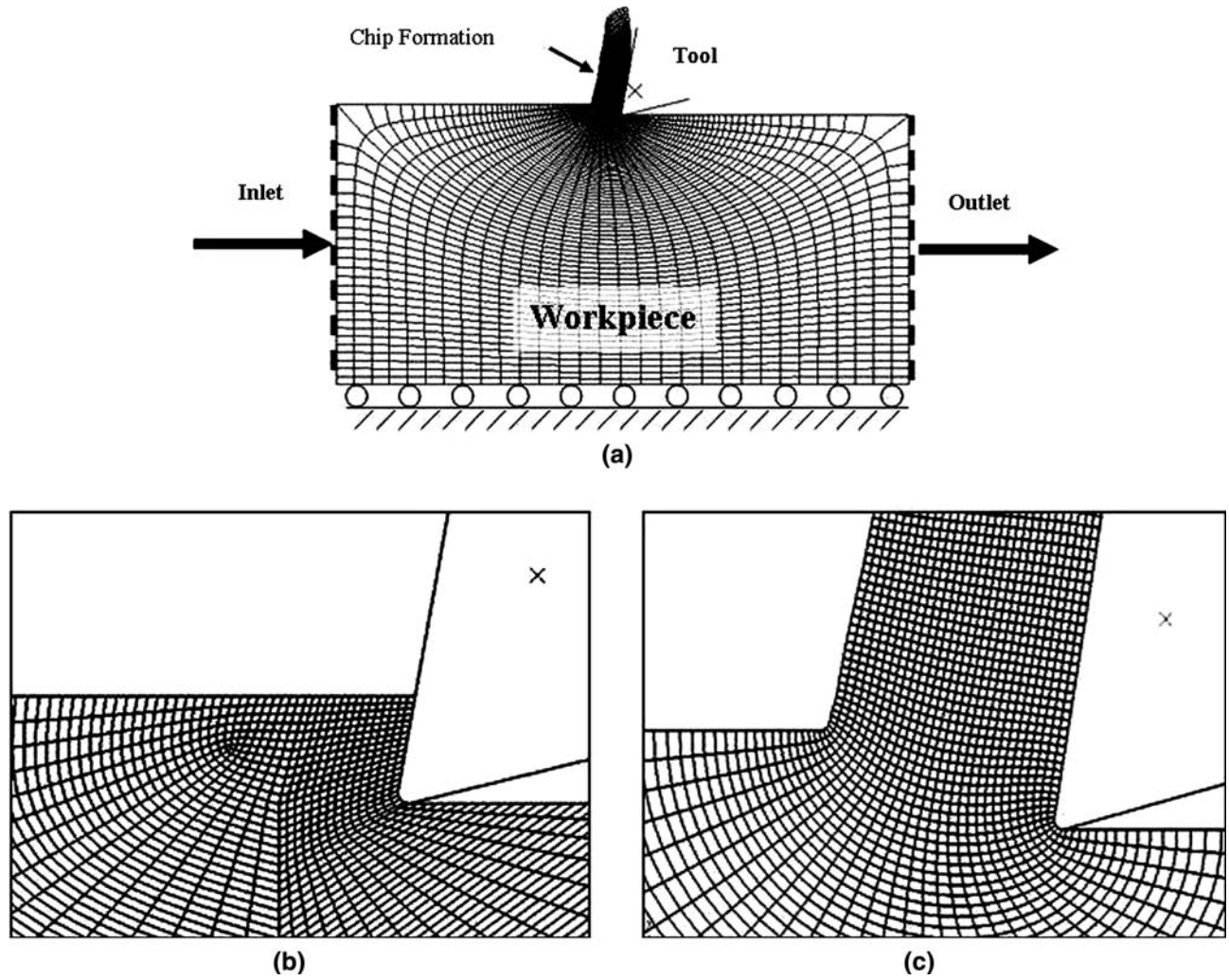

Fig. 4—Finite element model for plane strain machining ($\alpha = +10$ deg).

strain deformation at low speeds. A constant coefficient of friction (μ) is prescribed at the chip-tool interface. Lead is used as the model material system because of availability of material properties and experimental results pertaining to deformation in machining. ABAQUS/CAE* is used for arrangement of model

*ABAQUS/CAE is trademarked under ABAQUS, Inc., Providence, RI.

elements and nodes (Figure 4). The basic element used in the simulation is the isoparametric plane strain, 4 node, 8 degree of freedom quadrilateral with reduced integration.[39,40] The relative simplicity of this element expedites the computation run time of the simulation with minimal loss of accuracy, for the class of examples studied here.

In order to accommodate the extreme plastic deformation encountered, ABAQUS/Explicit** is used to

**ABAQUS/Explicit is trademarked under ABAQUS, Inc., Providence, RI.

solve the proposed nonlinear dynamic analysis. This solver is based on a central explicit integration rule implemented together with diagonal or "lumped" mass matrices.[41,42] Although this method employs a great number of small increments, the simplicity of the matrix computation offers reduced simulation run time compared to standard finite element solvers.

Further promotion of finite element efficiency in explicit formulation is achieved through "mass scaling." This procedure allows the minimum stable time increment to be artificially increased through augmentation of the mass density of the material.[40,42] This is common in finite element simulations where inertial effects are negligible (usually "slow" processes).[33]

Perhaps the most significant obstacle in finite element modeling of machining is preserving the integrity of the mesh throughout the chip formation process. As described earlier, adaptive meshing offers an enticing answer to this problem. The approach used here is a type of arbitrary Lagrangian Eulerian method described earlier.[33–37] For the majority of the analysis, the movement of the nodes is tied to the motion of the underlying material. However, a series of "remesh" increments are applied at equal intervals throughout the primarily Lagrangian simulation. During a remesh increment, nodes are relocated based on the current positions of neighboring nodes and elements to minimize distortion and keep the size of neighboring elements similar. The inlet and outlet surfaces of the workpiece (Figure 4) are designated as Eulerian boundaries. This means that the nodes lying along these boundaries, having moved out of place since their previous remesh, are realigned according to the imposed constraints during the ensuing remesh increment. The nodes along all other surfaces are allowed to traverse tangentially along but may not deviate from the

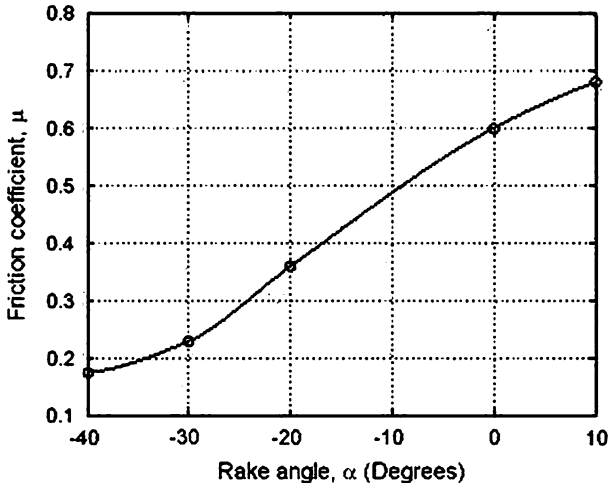

Fig. 5—Experimental friction values at the tool-chip interface.

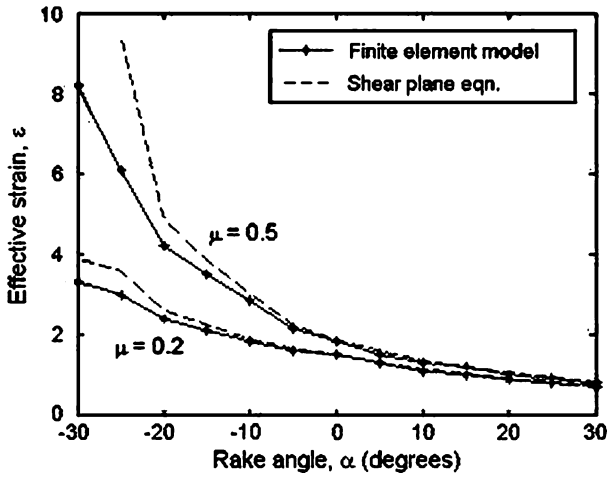

Fig. 6—Variation of effective strain in chip with rake angle for assumed conditions of dry (μ = 0.5) and lubricated (μ = 0.2) cutting.

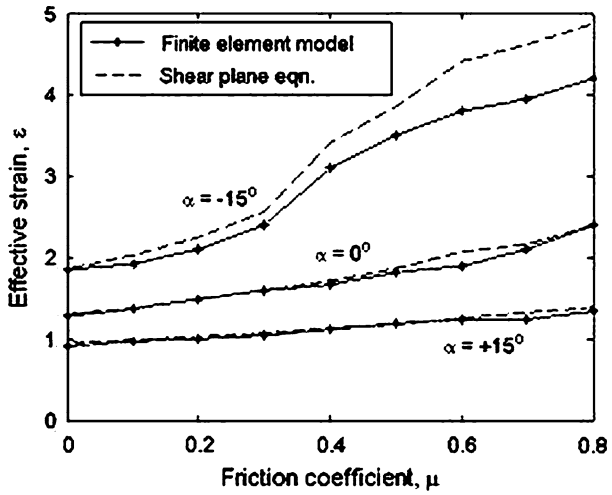

Fig. 7—Variation of effective strain in chip with friction coefficient for α = +15, 0, and −15 deg.

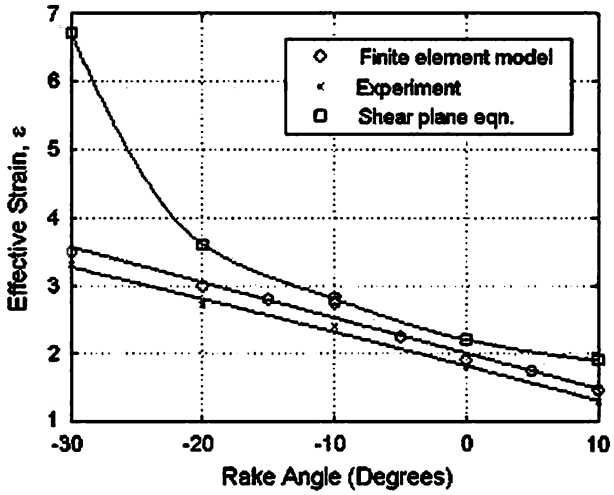

Fig. 8—Comparison of finite element simulation strain results with experiment for plane strain machining of lead.

material surface, thereby preserving the deformed chip geometry.

Solution variables are mapped from the old mesh to the new mesh following the remesh increment. The material added at the "inlet" Eulerian boundary at nodal remapping is assumed to be identical to the adjacent material. In order for numerical stability to occur, the difference between the old and new mesh must be small. Each adaptive mesh increment takes approximately three to five times the duration of a standard Lagrangian increment. In chip formation, these remeshing increments are only a small fraction of the total necessary, so the additional computational time due to adaptive meshing is negligible.

III. RESULTS

Models of plane strain machining such as the shear plane model and finite element formulations assume deformation is at a steady state (Figure 2(a)).[11–13] Although the chip length increases proportional to the length of cut, the deformed chip thickness, precut (undeformed) thickness, and cutting velocity all remain constant after deformation has reached steady state. Therefore the deformation zone should maintain a constant size and shape after a certain amount of incipient deformation. This assumption is incorporated into the current finite element model using Eulerian

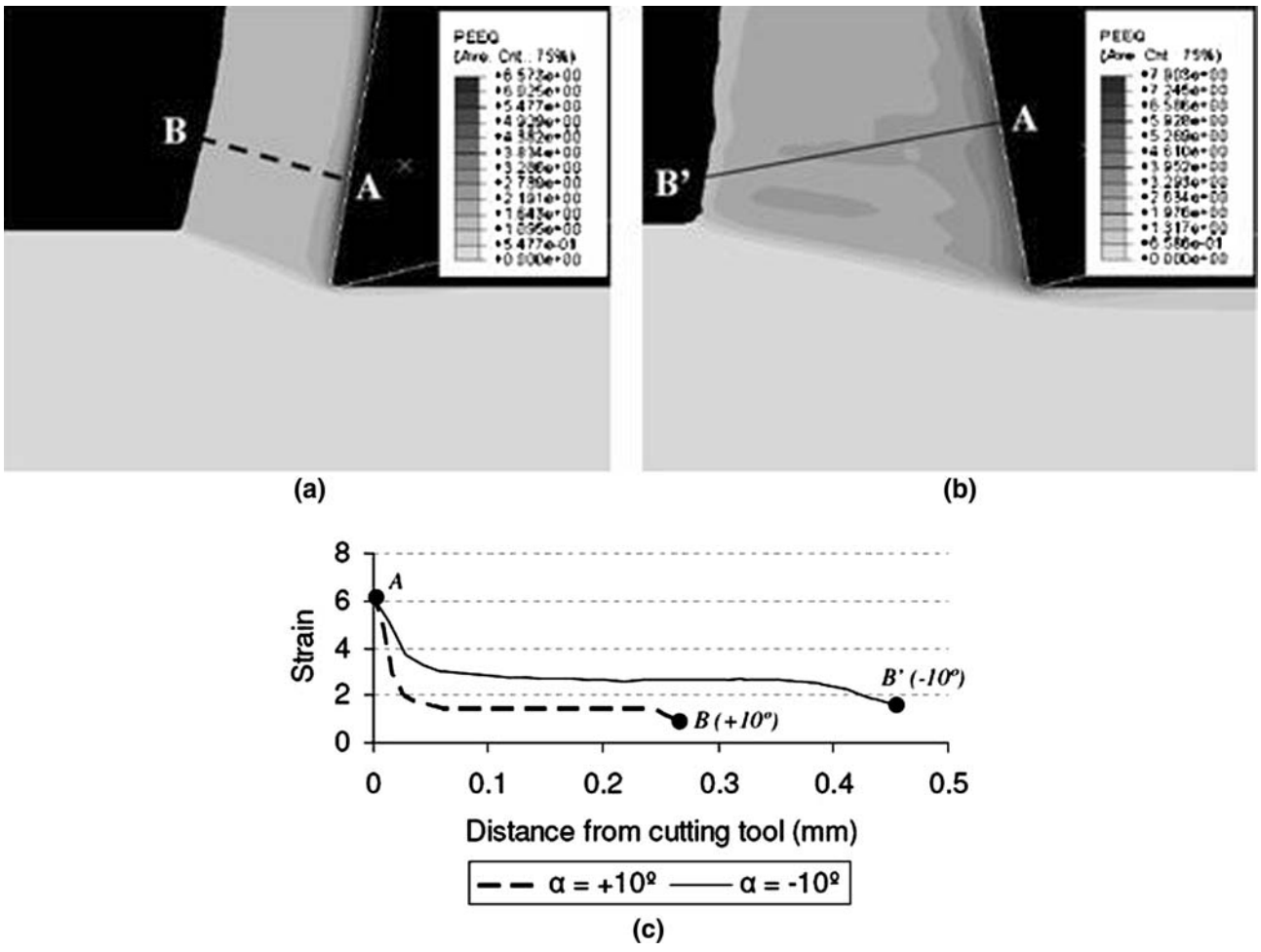

Fig. 9—Distribution of strain across chip thickness for cutting rake angles of (*a*) +10 and (*b*) −10 deg shown in contour plots of cumulative effective strain.

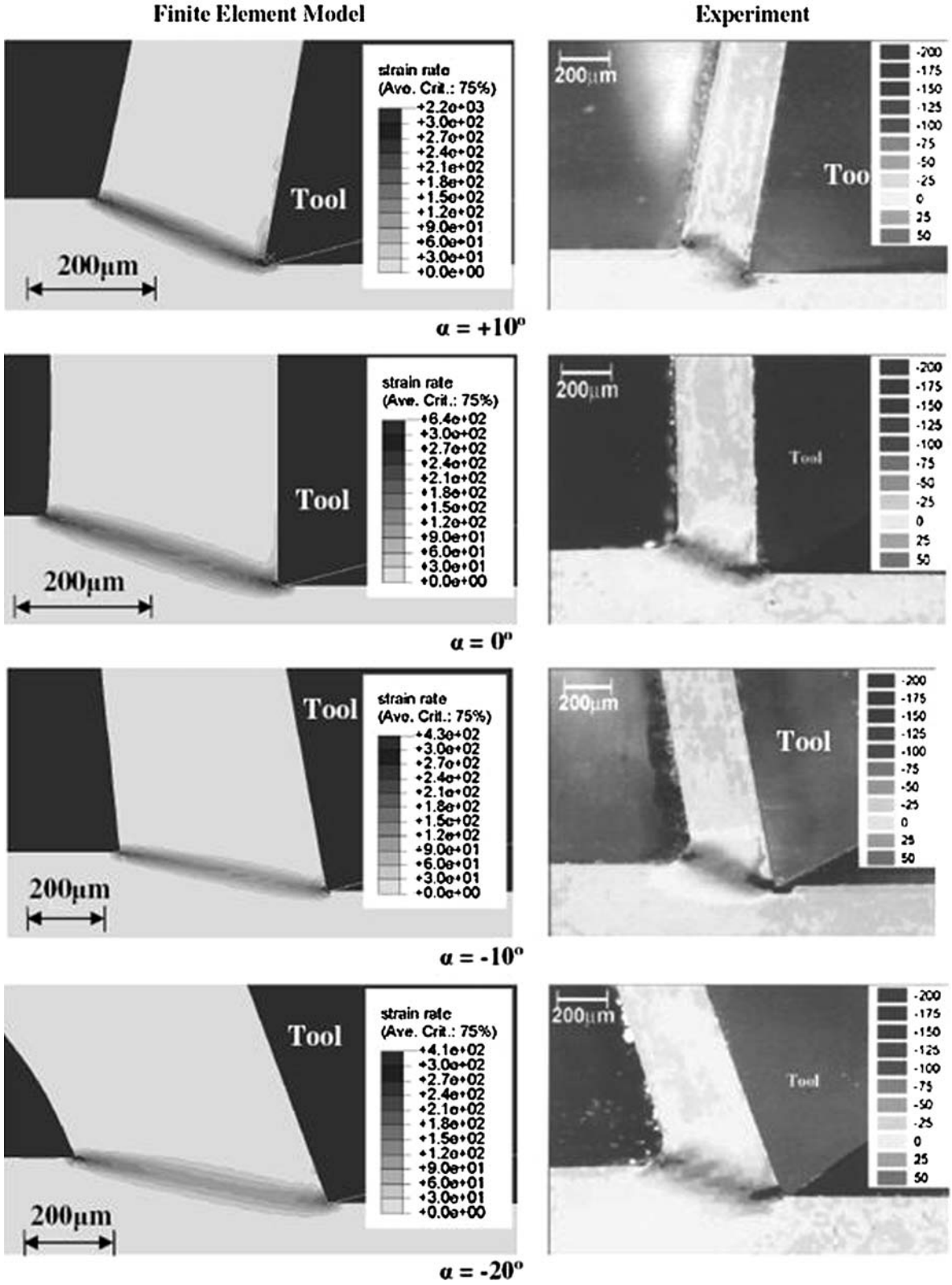

Fig. 10—Effective strain rate distributions for machining lead at different rake angles.

boundaries as the inlet and outlet surfaces (Figure 4), so that material may "flow through" the mesh at a prescribed cutting velocity. The bottom surface connecting the Eulerian boundaries is fixed vertically and experiences no deformation. The opposite surface forms a chip adjacent to the cutting tool as time

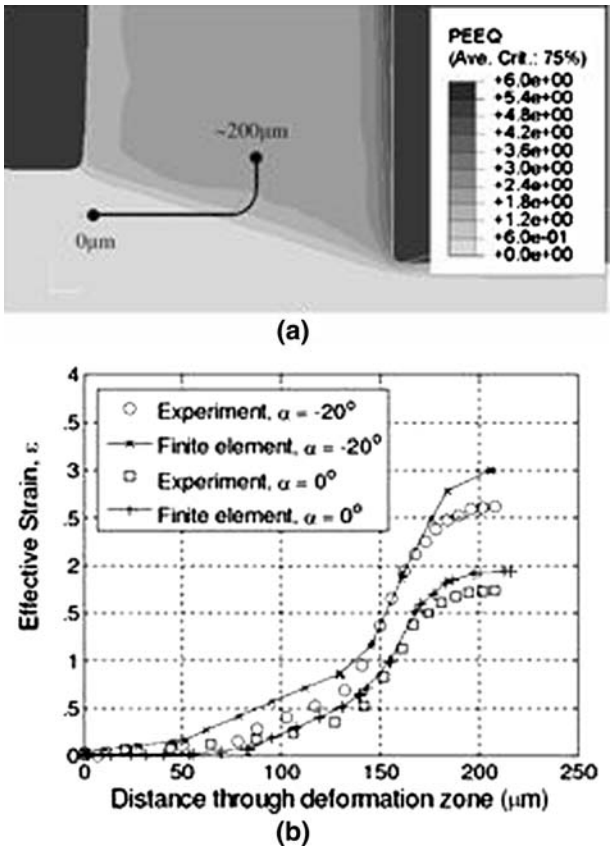

Fig. 11—Accumulation of strain as a particle moves from the undeformed workpiece into the chip (α = 0 deg, –20 deg).

progresses through the simulation. These two surfaces act as material boundaries while allowing nodes to "slide" tangentially. The mesh has been formulated to facilitate easy transition from the uncut workpiece to the fully developed chip.

Plane strain machining at low speeds was simulated for rake angles between –30 and +30 deg at 5 deg increments. The workpiece was assigned material properties characteristic of lead: Young's modulus of 13 GPa, Poisson's ratio of 0.44, and yield strength of 10 MPa with no strain hardening. The depth of cut was set at 100 μm (undeformed chip thickness), which also determines the other relative dimensions of the workpiece. The height (2.5 mm) and width (5 mm) of the modeled workpiece were taken to be much greater than the depth of cut so as to not interfere with the plastic deformation and to ensure a condition of plane strain. The radius of the tool tip was kept sufficiently small (10 μm) to represent a "sharp tip" akin to experimental conditions.

An important aspect in modeling of machining is the interaction between tool rake face and chip. The friction at this interface has a significant effect on chip morphology and shear strain associated with chip formation. In some models, a constant coefficient of friction is assumed to prevail along the entire contact length of the rake face while in others, the tool-chip contact region is decomposed into a "sticking" region near the tool tip and a "sliding" region away from the tool tip.[19] For the sake of simplicity, a constant value was assigned for the friction coefficient at the chip-tool interface in the present simulation. The value of this coefficient of friction was taken to be that measured in plane strain machining of lead. Figure 5 shows the measured coefficient of friction for the machining of lead by a sapphire cutting tool at various rake angles. Except where noted, the coefficient of friction values used in the finite element simulation for the different rake angles adhere to those shown in Figure 5.

It is of interest to initially compare the finite element simulation results for effective strain in chip with corresponding values estimated using the upper bound solution of the shear plane model. This comparison was done for two coefficient of friction values, 0.2 and 0.5, representative of lubricated and dry machining, respectively. For making this comparison, a representative value for the cumulative strain in the chip was estimated from the finite element results by evaluating the average strain throughout the central region of the chip thickness (so as not to include additional strain from friction at the tool-chip interface).

Figure 6 shows the variation of effective strain with rake angle thus determined using the finite element simulation for the two friction conditions. Corresponding values for the effective strain in the shear plane model were obtained by substituting chip thickness values from the finite element simulation into Eqs. [1] through [4]. This comparison shows that the finite element strain results compare well against the shear plane model for positive rake angles but diverge at negative rake angles (Figure 6). The value of the finite element shear strain is seen to increase with decreasing rake angle (*i.e.*, as the rake angle becomes more negative or less positive) consistent again with the prediction of the shear plane model. The effective strain for a given rake angle is also seen to increase significantly with friction for a range of assumed friction coefficients (Figure 7). Here again the finite element results diverge from the shear plane model as the rake angle becomes more negative and with increasing friction. Figures 6 and 7 demonstrate the powerful capability afforded by the finite element simulation in predicting the deformation (*e.g.*, strain) as a function of the machining parameters.

The finite element simulation results for strain can be compared directly with strain values estimated from an experiment using the particle image velocimetry technique,[8] by using the measured coefficient of friction values for the plane strain machining in the simulation (Figure 5). In experiments, the friction coefficient decreases significantly as the rake angle becomes less positive (Figure 5). When this information is incorporated into the simulation, the predicted finite element strain results are seen to be in close agreement with the strain values determined from experiment (Figure 8). For comparison, the shear plane model strains for the same friction conditions are also shown in Figure 8. The improved strain prediction at the more negative rake angles offered by the finite element model may be noted.

Figure 9 shows the strain distribution across the thickness of the chip thickness. From Figure 9(c), it is

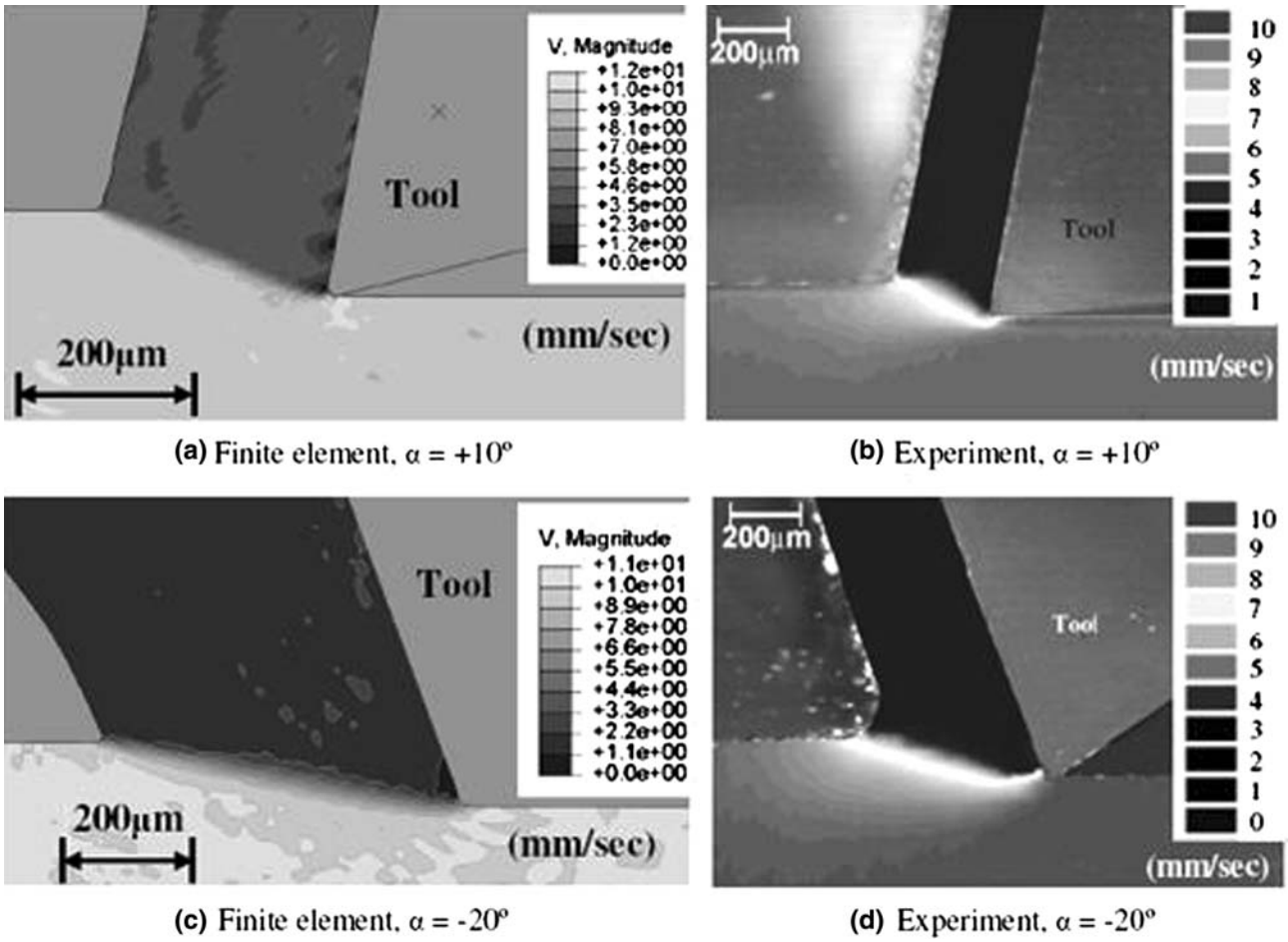

Fig. 12—Velocity profiles for low speed (V_o = 10 mm/s) cutting of lead (α = +10 deg, –20 deg).

clear that the cumulative strain is relatively uniform over most of the thickness. A significant increase in the strain, however, is observed near the rake face of the tool, "A." This is a consequence of additional straining arising from the friction at the tool-chip interface. Such friction-induced deformation is prevalent in all metal deformation processes, including severe plastic deformation methods like equal channel angular pressing. While this is likely to induce some additional refinement of the microstructure in this region of secondary deformation, the microstructure over the bulk of the thickness of the chip is uniform as established by orientation imaging microscopy and transmission electron microscopy.[9] This is consistent with the relatively uniform distribution of strain in the chip shown in Figure 9. Therefore, the cumulative strain value estimated in the center of the chip may be assumed to be representative of the strain in the chip as a whole.

The strain rate contours in chip formation produced by the finite element simulation indicate a narrow band within which the most of the deformation occurs while the experimental results indicate a slightly broader region of deformation (Figure 10). Upon closer inspection of the experimental results in Figure 10(b), it can be noted that relatively lower strain rates ($< 50\ s^{-1}$) prevail over most of this deformation region while the higher strain rates ($> 100\ s^{-1}$) occur within a narrow band that is approximately the same size and shape as that predicted by the finite element simulation. This concentration of strain rate in the deformation zone is perhaps even better seen in Figure 11, where the cumulative effective strain of a particle is mapped as it moves from the undeformed workpiece into the fully developed chip, through the deformation zone. It should be noted that the highest strain rates in all cases shown in Figure 10 occur at either extremities of the deformation zone, near the tool tip (cutting edge) and at the other end of the deformation zone adjoining the free surface. Figure 10 also indicates a secondary region of deformation at the tool-chip interface due to frictional forces, consistent with prior observations of this region in machining.[11,10]

Figure 12 shows velocity distributions obtained from the finite element simulation and experimentally *via* PIV analysis.[8] These indicate that the velocity throughout the chip is uniform and related to the cutting velocity by the ratio of the undeformed to deformed chip thickness (Figure 12), as expected. More importantly, the transition from the bulk to the chip velocity is seen to occur over a narrow region that corresponds to the deformation zone described in Figure 10. In situations where significant strain is imposed in the chip, as when machining with highly negative rake angle tools, the

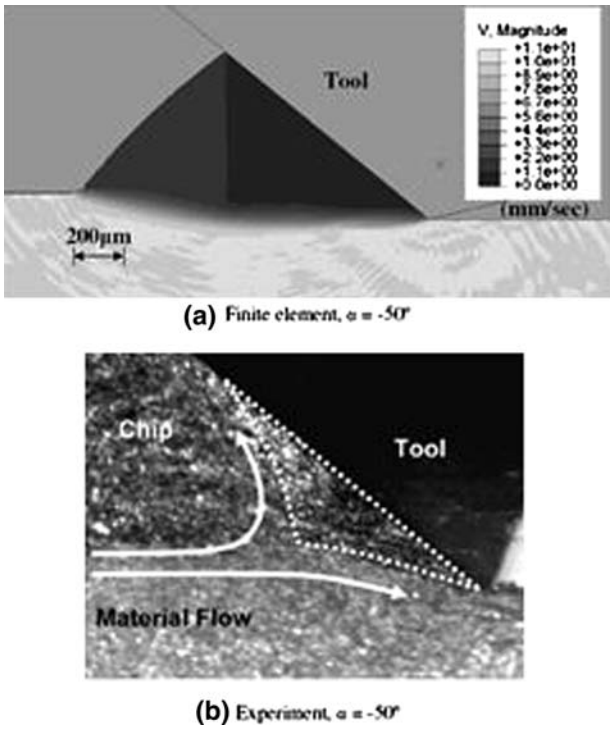

Fig. 13—The buildup of stagnant dead metal at the tool tip for $\alpha = -50$ deg.

friction forces the chip material adjacent to the tool rake face to ''stick'' to this face. For some rake angles, this stuck material may be seen as a small extension of the tool tip (Figure 12, $\alpha = -20$ deg), where the adjoining material bypasses the ''stuck'' material by plastically flowing around it. This stuck region of ''dead metal'' allows material to build up ahead of the tool tip; the dead metal region is commonly referred to as a built-up edge in machining.[12] Figure 13(a) shows a particularly extreme example of the formation of a dead metal region when cutting with a −50 deg rake angle tool. The finite element simulation predicts infeasibility of continuous chip formation for this condition and instead a pileup of work material ahead of the tool tip. This rake angle may be identified as the critical rake angle below which no chip formation is possible. Such a lack of chip formation has indeed been observed in plane strain machining of lead under similar conditions (Figure 13(b)).

IV. CONCLUDING REMARKS

The finite element model of machining described here is a key element in establishing plane strain machining as a controlled method of severe plastic deformation and as a process for making ultra-fine-grained materials. By characterizing the dependence of the shear strains and strain rates in the deformation zone, on the tool rake angle and friction at the tool-chip interface, an important step has been taken in relating the machining input parameters to the deformation parameters (*e.g.*, strain and strain rate). Such a correlation is necessary for establishing machining as an experimental framework in which to systematically study the manifold and interactive effects of large strain deformation (*e.g.*, strain and strain rate) on microstructure and properties of materials. A comparison of shear strains and their distributions in the deformation zone estimated using the finite element model with direct measurements of these strain fields in plane strain machining has shown more than reasonable agreement, with further validation studies in progress. The simulation has also shown that the strain field can be varied over a wide range by appropriate control of machining input parameters. Taken together, these results establish the feasibility of machining as a robust and efficient method of severe plastic deformation even for difficult-to-deform materials at ambient temperature. Finally, the finite element simulation has provided a characterization of some machining conditions that inhibit chip formation; this prediction is again found to be consistent with direct observations of chip formation.

Prior studies of microstructure of machining chips have confirmed the occurrence of nanoscale and ultra-fine-grained microstructures and their specific dependence on deformation field parameters. By incorporating microstructure-based models into our current model of mechanics of large strain deformation in chip formation, it will likely be feasible to predict the right combinations of parameters needed to create ultra-fine-grained alloys with desired microstructure and properties. The mechanics of microstructure evolution at different length scales could then also be elucidated. These, together with refinement of our present finite element model to include temperature influences, offer much scope for further study.

ACKNOWLEDGMENTS

We acknowledge NASA GSRP Fellowship No. NND04CR12H and NSF Grant Nos. CMS-0200509, CMMI-0626047 and CMMI-0626541 in support of this work. We also thank Dr. Srinivasan Swaminathan, Naval Post Graduate School (Monterrey, CA), previously at Purdue, for his contributions to this work.

REFERENCES

1. R.Z. Valiev, A.V. Korznikov, and M.M. Mulyukov: *Mater. Sci. Eng. A*, 1993, vol. 168, pp. 141–48.
2. F.J. Humphreys, P.B. Prangnell, J.R. Bowen, A. Gholinia, C. Harris, J. Gil Sevillano, C. Garcia-Rosales, and J. Flaquer-Fuster: *Philos. Trans. R. Soc. London, Ser. A*, 1999, vol. 357, pp. 1663–81.
3. M. Furukawa, Z. Horita, M. Nemoto, and T.G. Langdon: *J. Mater. Sci.*, 2001, vol. 36, pp. 2835–43.
4. J.D. Embury and R.M. Fisher: *Acta Metall.*, 1966, vol. 14, pp. 147–59.
5. G. Langford and M. Cohen: *Trans. ASM*, 1969, vol. 62, pp. 623–38.
6. V.M. Segal, V.I. Reznikov, A.E. Drobyshevskiy, and V. Kopylov: *Russ. Metall.*, 1981, vol. 1, pp. 99–105.
7. T.L. Brown, S. Swaminathan, S. Chandrasekar, W.D. Compton, A.H. King, and K.P. Trumble: *J. Mater. Res.*, 2002, vol. 17, pp. 2484–88.
8. M. Ravi Shankar, B.C. Rao, S. Lee, S. Chandrasekar, A.H. King, and W.D. Compton: *Acta Mater.*, 2006, vol. 54, pp. 3691–3700.

9. S. Swaminathan, T.L. Brown, S. Chandrasekar, T.R. McNelley, and W.D. Compton: *Scripta Mater*., 2007, vol. 56, pp. 1047–50.
10. S. Lee, J. Hwang, M. Ravi Shankar, S. Chandrasekar, and W.D. Compton: *Metall. Mater. Trans. A*, 2006, vol. 37, pp. 1633–43.
11. M.C. Shaw: *Metal Cutting Principles*, Oxford University Press, Oxford, United Kingdom, 1984.
12. P.L.B. Oxley: *The Mechanics of Machining: An Analytical Approach to Assessing Machinability*, John Wiley & Sons, New York, NY, 1989.
13. S. Kobayashi and E.G. Thomsen: *J. Eng. Ind.*, 1960, vol. 81, pp. 251–62.
14. P.V. Desai and S. Ramalingam: *J. Eng. Ind.*, 1981, vol. 103, pp. 79–80.
15. B.E. Klamecki: Ph.D. Thesis, University of Illinois at Urbana–Champaign, Urbana, IL, 1973.
16. T. Shirakashi and E. Usui: *Proc. Int. Congr. Prod. Eng., Tokyo*, 1974, pp. 535–40.
17. J.S. Strenkowski and J.T. Carroll: *J. Eng. Ind.*, 1985, vol. 107, pp. 349–54.
18. K. Iwata, K. Oskada, and Y. Terasaka: *J. Eng. Mater. Technol.*, 1974, vol. 106, pp. 132–38.
19. A.J.M. Shih, S. Chandrasekar, and H.T.Y. Yang: *ASME Pub. PED*, 1990, pp. 11–24.
20. K. Komvopoulos and S.A. Erpenbeck: *J. Eng. Ind.*, 1991, vol. 113, pp. 253–67.
21. Z.C. Lin, K.T. Chu, and W.C. Pan: *J. Mater. Process. Technol.*, 1994, vol. 41, pp. 291–310.
22. B. Zhang and A. Bagchi: *J. Eng. Ind.*, 1994, vol. 116, pp. 289–97.
23. H. Ernst: *Machining of Metals*, American Society of Metals, Cleveland, OH, 1938.
24. I. Finnie: *Mech. Eng.*, 1956, vol. 78, pp. 715–21.
25. A.J.M. Shih: *Int. J. Mech. Sci.*, 1996, vol. 38, pp. 1–17.
26. J.T. Carroll and J.S. Strenkowski: *Int. J. Mech. Sci.*, 1988, vol. 30, pp. 899–920.
27. G.S. Sekhon and J.L. Chenot: *Eng. Comp.*, 1993, vol. 10, pp. 31–48.
28. I.S. Jawahir, A.K. Balaji, R. Stevenson, and C.A. van Luttervelt: *Symp. Predictable Modeling in Metal Cutting as Means of Bridging Gap between Theory and Practice*, Manufacturing Science Technology, American Society of Mechanical Engineers (ASME) International Mechanical Engineering Conference and Exposition (IMECE), ASME, New York, NY, MED-6-2, 1997, pp. 3–12.
29. C.A. van Luttervelt , T. Childs, I.S. Jawahir, and F. Klocke: *Ann. CIRP*, 1998, vol. 47, pp. 587–626.
30. E. Ceretti, P. Fallböhmer, W.T. Wu, and T. Altan: *J. Mater. Process. Technol*, 1996, vol. 59, pp. 169–80.
31. A. Simoneau, E. Ng, and M.A. Elbestawi: *Ann. CIRP*, 2006, vol. 55, pp. 97–102.
32. E. Uhlmann, M. Graf von der Schulenburg, and R. Zettier: *Ann. CIRP*, 2007, vol. 56, pp. 61–64.
33. T.D. Marusich and M. Ortiz: *Int. J. Num. Meth. Eng.*, 1995, vol. 38, pp. 3675–94.
34. V. Madhavan, S. Chandrasekar, and T.N. Farris: *J. Appl. Mech.*, 2000, vol. 67, pp. 128–39.
35. J. Hashemi and R. Stefan: *Recent Advances in Structural Mechanics*, American Society of Mechanical Engineers (ASME), Pressure Vessels and Piping Conference (PVP), ASME, New York, NY, 1994, vol. 295, pp. 113–25.
36. L. Olovsson, L. Nilsson, and K. Simonsson: *Comput. Struct.*, 1999, vol. 72, pp. 497–507.
37. M.R. Movahhedy, M.S. Gadala, and Y. Altintas: *Mach. Sci. Technol.*, 2000, vol. 4, pp. 15–42.
38. M. Sevier, S. Lee, M.R. Shankar, H.T.Y. Yang, S. Chandrasekar, and W.D. Compton: *Mater. Sci. Forum*, 2006, vols. 503–504, pp. 379–84.
39. I.C. Taig: English Electric Aviation Report, S017, England, 1961.
40. D.P. Flanagan and T. Belytschko: *Int. J. Num. Meth. Eng.*, 1981, vol. 17, pp. 679–706.
41. M. Kleiber: *Incremental Finite Element Modeling in Non-Linear Solid Mechanics*, John Wiley & Sons, New York, NY, 1989.
42. ABAQUS: *ABAQUS Theory Manual*, Version 6.5, Hibbitt, Karlsson & Sorenson, Inc, Pawtucket, RI, 2004.
43. D.J. Benson: *Comp. Meth. Appl. Mech. Eng.*, 1989, vol. 72, pp. 305–50.